Quantum electrodynamics in three dimensions: Dynamical chiral symmetry breaking, confinement, and disorder effects

Guo-Zhu Liu, Hua Jiang, Wei Li, and Geng Cheng
Department of Modern Physics, University of Science and Technology of China, Hefei, Anhui 230026, People's Republic of China
(Received 22 August 2008; published 7 January 2009)

We study dynamical chiral symmetry breaking (DCSB), confinement, and disorder effects in $(2+1)$-dimensional quantum electrodynamics (QED) of massless fermion ψ and scalar boson ϕ. It is found that gauge symmetry breaking (GSB) induced by nonzero $\langle\phi\rangle$ rapidly suppresses the occurrence of DCSB, and certain disorders tend to enhance it. While DCSB leads to confinement in the gauge symmetric state, the matter fields are always deconfined in the GSB state whether chiral symmetry is broken or not. According to the symmetries and the classical potential between particles, QED_3 has three possible phases, which exhibit distinct phenomena and can be identified by appropriate observable quantities.

DOI: 10.1103/PhysRevB.79.014507 PACS number(s): 74.20.Mn, 11.10.Kk, 11.15.Ex, 11.15.Pg

Three-dimensional quantum electrodynamics (QED_3) exhibits very interesting properties such as spontaneous (dynamical) symmetry breaking and confinement (CM). It also has extensive applications in planar condensed-matter physics. In particular, the low-energy physics of high-temperature superconductors can be described by QED_3 of massless Dirac fermion and scalar boson.[1–5] In this case, the spin and charge degrees of freedom of electrons are separated with spin and charge represented by massless fermion and scalar boson, respectively.[1] The gauge field emerges as the result of strong electron correlation and is not the usual electromagnetic field.[1]

The effective theory has two continuous symmetries: local gauge symmetry and chiral symmetry. However, they both can be broken spontaneously or dynamically. The gauge symmetry is spontaneously broken when the scalar field develops a nonzero vacuum expectation value corresponding to the phase transition to superconductivity.[1] The gauge boson then becomes massive via the Anderson-Higgs mechanism. The chiral symmetry can be dynamically broken by a finite fermion mass, which is usually generated through strong gauge interaction.[6–9] These two kinds of symmetry breaking are not independent. In fact, the mass m_a of gauge boson generated by gauge symmetry breaking (GSB) weakens the gauge interaction and thus can suppress the happening of dynamical chiral symmetry breaking (DCSB).[10]

In any realistic many-body system, there are always disorders of various types. Disorders can bring a plethora of interesting phenomena such as localization and metal-insulator transition.[11] However, how they affect DCSB has not been systematically studied. In this paper, we study the effects of gauge interaction and disorders on DCSB in QED_3. By incorporating disorders into the Dyson-Schwinger (DS) integral equation of fermion self-energy, we found that DCSB is suppressed by growing gauge boson mass m_a but is enhanced by growing disorder strength g. As a consequence of this competing effect, there is a critical line in the m_a-g plane which separates the DCSB phase and the chiral-symmetric phase.

Confinement is another interesting property of QED_3.[12–14] In the state where local gauge symmetry is preserved, the massless fermions are deconfined but are confined by a logarithmically growing classical potential once DCSB takes place.[13,14] In this paper, we show that the close correspondence between DCSB and confinement is destroyed by GSB. Actually, the matter fields are always deconfined in the superconducting state irrespective of the mass of fermions.

According to whether the chiral and gauge symmetries are preserved or broken, and to whether the matter fields are confined or deconfined, the whole system can stay in three possible phases. The system exhibits quite different physical properties in each of these phases, so we can identify each phase by theoretical and experimental investigations of some observable quantities. We present the phase diagram of the system and show how to identify each phase by the thermal conductivity.

We start with the Lagrangian $\mathcal{L}=\mathcal{L}_F+\mathcal{L}_B$, where

$$\mathcal{L}_F=-\frac{1}{4}F_{\mu\nu}F^{\mu\nu}+\sum_{\sigma=1}^{N}\bar{\psi}_\sigma(\partial_\mu-iea_\mu)\gamma_\mu\psi_\sigma, \tag{1}$$

$$\mathcal{L}_B=\sum_{i=1}^{2}|(\partial_\mu-iea_\mu)\phi_i|^2+\mu^2\phi^2+\lambda\phi^4. \tag{2}$$

Here, $\mathcal{L}_F$ describes the interaction between massless Dirac fermions ψ and gauge field a_μ (Ref. 15), and $\mathcal{L}_B$ is the relativistic Ginzburg-Landau model.[16] The 4×1 spinor ψ_σ represents the massless Dirac fermion. Its conjugate field is defined as $\bar{\psi}=\psi^\dagger\gamma_0$. The 4×4 γ_μ matrices obey the Clifford algebra, $\{\gamma_\mu,\gamma_\nu\}=2\delta_{\mu\nu}$. The fermion has flavor N, whose physical value is 2.[1,2] The flavor of scalar field ϕ is taken to be 2, but the extension to other flavors is straightforward.

The propagator of free Dirac fermion is simply $S_0^{-1}(p)=i\gamma\cdot p$, while the full inverse fermion propagator is given by $S^{-1}(p)=i\gamma\cdot pA(p^2)+\Sigma(p^2)$, where $A(p^2)$ is the wave-function renormalization and $\Sigma(p^2)$ is the fermion self-energy function. The full and bare fermion propagators are related by the DS equation

$$S^{-1}(p)=S_0^{-1}(p)+\int\frac{d^3k}{(2\pi)^3}\gamma^\mu S(k)D_{\mu\nu}(p-k)\Gamma^\nu(k,p).$$

Here the fermion self-energy diagram is shown in Fig. 1, where the internal solid line is the full fermion propagator

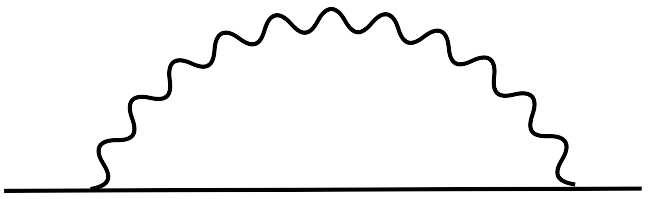

FIG. 1. The lowest-order fermion self-energy correction arising from gauge interaction.

and the wavy line is the gauge boson propagator.

If the DS equation for fermion self-energy $\Sigma(p^2)$ has only vanishing solutions, the fermions are massless and the Lagrangian respects the chiral symmetry $\psi \to \exp(i\beta\gamma_{3,5})\psi$, with 4×4 matrix $\gamma_{3,5}$ anticommuting with γ_μ $(\mu=0,1,2)$. Once the DS equation develops a squarely integrable nontrivial solution, the massless fermions acquire a finite mass. The complete DS equation is extremely complicated, and it is necessary to make proper approximations. To the lowest order of $1/N$ expansion, we assume that $A(p^2)=1$ and approximate the vertex function $\Gamma_\mu(k,p)$ by bare vertex γ_μ.[6] Thus the DS equation simplifies to

$$\Sigma(p^2) = e^2 \int \frac{d^3k}{(2\pi)^3} \frac{\gamma^\mu D_{\mu\nu}(p-k)\Sigma(k^2)\gamma^\nu}{k^2+\Sigma^2(k^2)}. \tag{3}$$

The gauge boson propagator in the Landau gauge is

$$D_{\mu\nu}(q) = \frac{1}{q^2[1+\Pi(q)]+m_a^2}\left(\delta_{\mu\nu} - \frac{q_\mu q_\nu}{q^2}\right), \tag{4}$$

where $\Pi(q)$ is the vacuum polarization function and m_a is the mass of gauge boson (defined later). The polarization function $\Pi(q)$ contains two contributions: $\Pi(q)=\Pi_F(q)+\Pi_B(q)$ where $\Pi_F(q)=\alpha/8|q|$ is the fermion contribution[6] with $\alpha=Ne^2$ being fixed as $N\to 0$ and $\Pi_B(q)$ is the scalar boson contribution. In the absence of scalar boson, $\Pi_B(q)=0$, DCSB takes place once the fermion flavor N is less than a critical value N_c which is $32/\pi^2$ to the lowest order.[6–9] The physical fermion flavor is $N=2<N_c$, so DCSB actually happens and the fermions become massive. In the presence of nonzero $\Pi_B(q)$, this result is changed.

We now consider the Lagrangian $\mathcal{L}_B$. If $\mu^2>0$, the scalar field ϕ has a vanishing vacuum expectation value of $\langle\phi\rangle=0$ and the Lagrangian is invariant under local gauge transformation $\phi(x)\to e^{i\theta(x)}\phi(x)$. If $\mu^2<0$, ϕ develops a finite vacuum expectation value of $\langle\phi\rangle=v/\sqrt{2}$ with $v=\sqrt{-\mu^2/\lambda}$. The nonzero $\langle\phi\rangle$ spontaneously breaks the continuous local gauge symmetry and hence would lead to a massless Goldstone boson. However, the Goldstone boson can be eliminated by a particular gauge transformation, generating a finite gauge boson mass. To calculate the polarization $\Pi_B(q)$, we decompose the scalar field as $\phi(x)=[v+h(x)+i\varphi(x)]/\sqrt{2}$ so that the boson Lagrangian can be rewritten in the form

$$\mathcal{L}_B = \frac{1}{2}(\partial_\mu h)^2 + \frac{1}{2}(\partial_\mu\varphi)^2 + \frac{1}{2}e^2(v+h)^2a_\mu^2 + \frac{1}{2}e^2\varphi^2a_\mu^2 + e\varphi a^\mu\partial_\mu h - e(v+h)a^\mu\partial_\mu\varphi - \frac{\lambda}{4}(h^4+\varphi^4+4v^2h^2+4vh^3+4vh\varphi^2+2h^2\varphi^2).$$

It is easy to see that the mass of Higgs scalar boson is $m_h=\sqrt{2\lambda}v$ and the mass of gauge boson is $m_a=ev$. Either of them can be used as the turning variable to study how N_c varies. The ratio $r=m_h/m_a=\sqrt{2\lambda}/e$ is the Ginzburg parameter. The one-loop vacuum polarization $\Pi_B(q)$ contains four Feynman diagrams,[17,18] which gives rise to

$$\Pi_B = \frac{e^2}{4\pi q^2}\left[m_a - m_h + \frac{m_a}{q^2}(m_h^2-m_a^2) + \frac{m_h}{q^2}(m_a^2-m_h^2)\right] + \frac{e^2}{4\pi}\frac{(q^2+m_h^2-m_a^2)^2-4m_a^2q^2}{2q^5}\zeta, \tag{5}$$

where $\zeta=\arctan\frac{q^2+m_a^2-m_h^2}{2m_hq}+\arctan\frac{q^2+m_h^2-m_a^2}{2m_aq}$. In the absence of disorders, the DS equation can be solved numerically with the result that gauge boson mass m_a (and m_h) suppresses the critical fermion flavor N_c.[18]

We now include static disorders to the field theory. The random potential $U(\mathbf{x})$ induced by disorders has two consequences: it modifies the value of critical fermion flavor N_c, and it leads to a finite scattering rate (inverse scattering time) for fermions and produces finite physical quantities that can be measured by experiments. For the convenience of performing functional integration, we write down the action, rather than the Lagrangian, for the interaction between disorder and Dirac fermions,

$$S_{\text{dis}} = \int d^2\mathbf{x}dt \sum_{\sigma=1}^{N} U(\mathbf{x})\bar{\psi}_\sigma(x)\gamma_0\psi_\sigma(x). \tag{6}$$

The coupling between scalar boson field ϕ and random potential $U(\mathbf{x})$ is omitted since we are mainly interested in the single-particle spectrum of fermions. We assume the random potential $U(\mathbf{x})$ to be a Gaussian white noise so that $\langle U(\mathbf{x})\rangle=0$ and $\langle U(\mathbf{x})U(\mathbf{x}')\rangle=G\delta(\mathbf{x}-\mathbf{x}')$ where the mean value is taken with the distribution $P[U]=\exp[-\frac{1}{2G}\int d^2\mathbf{x}U^2(\mathbf{x})]$. To average over the random variable $U(\mathbf{x})$, we use the standard replica trick and perform a Hubbard-Stratonovich transformation,[11]

$$\int \mathcal{D}U \exp\left[-\int d^2\mathbf{x}\left(\frac{1}{2G}U^2 + \int dt U\bar{\psi}\gamma_0\psi\right)\right] = \exp\left[\frac{G}{2}\int d^2\mathbf{x}dtdt'\sum_{\alpha,\sigma}(\bar{\psi}_{\alpha,\sigma}\gamma_0\psi_{\alpha,\sigma})^2\right], \tag{7}$$

where G plays the role of a coupling constant. There appears an effective four-fermion action. The summation is over both the spin index σ and the replica index $\alpha=1,2,\ldots,R$. In the final step, we should take the limit $R\to 0$. To explore the localization properties, one usually can map this to an effective nonlinear σ model[11] after a series of manipulations. Then the fermion localization and metal-insulator transition

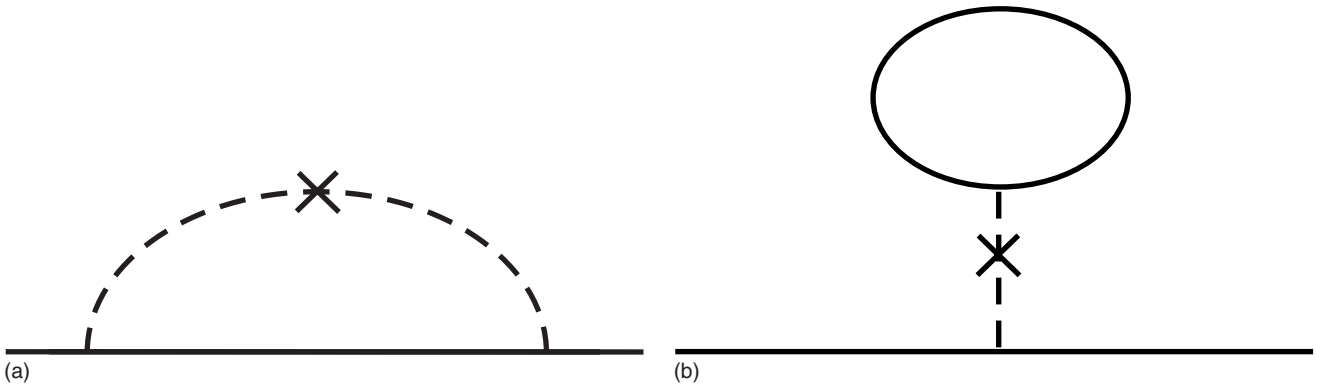

FIG. 2. (a) Allowed self-energy diagram in the lowest order. (b) Disallowed self-energy diagram. The dashed line represents disorder scattering.

can be analyzed systematically[11] using the renormalization group. Since we are only concerned in the single-particle spectrum of Dirac fermion, it is more convenient to deal with the four-fermion interaction (7). Notice that the whole action preserves the chiral symmetry. In fact, action (7) can be considered as a variant of the Nambu-Jona-Lasinio model,[19] which is known to be renormalizable and able to trigger DCSB in both (1+1) (Ref. 20) and (2+1) dimensions.[21] When there are no gauge and Coulomb interactions, the random Dirac fermion problem and the replicated action similar to (7) have been extensively studied in references,[22] focusing on the properties related to localization. We currently only consider the possibility of dynamical generation of fermion mass and simply ignore the localization effects.

Both gauge and four-fermion interactions can cause dynamical fermion mass generation and hence will be treated simultaneously. The Feynman rules[23] for impurity scattering have two novel features. First, the impurity lines carry only momentum and no energy because there is no energy transfer during the scattering of fermions by static disorders. Second, the impurity lines should always appear in pairs, which is a result of the Gaussian distribution of random potential $U(\mathbf{x})$. The lowest self-energy contribution to fermion propagator contains two diagrams (see Fig. 2). In the replica limit $R\to 0$, the diagram (b) vanishes since it has a closed fermion loop which leads to an extra factor R. The diagram (a) gives the only disorder contribution to fermion self-energy.

The DS equation for fermion mass function $\Sigma(p^2)$ is given by Eq. (3) when the fermions receive self-energy correction only from the gauge interaction. The effective four-fermion interaction (7) yields an additional contribution to Eq. (3), changing the DS equation to

$$\Sigma(p) = \frac{2\alpha}{N}\int \frac{d^3k}{(2\pi)^3}\frac{\Sigma(k)}{k^2+\Sigma^2(k)}\frac{1}{(p-k)^2[1+\Pi(|p-k|)]+m_a^2} + g\int \frac{d^2\mathbf{k}}{(2\pi)^2}\frac{\Sigma(k)}{p_0^2+\mathbf{k}^2+\Sigma^2(k)}, \tag{8}$$

where $g=GN$. In the right-hand side of this equation, the first term comes from the gauge interaction (Fig. 1) and the second term from the disorder effects [Fig. 2(a)]. Here we keep only the leading order of $1/N$ expansion and neglect all vertex corrections. Notice that in the second term the integration is taken over only momenta for the reason that the fermions do not exchange energy when scattered by static disorders.

Equation (8) is a nonlinear integral equation of the Hammerstein type. We can obtain the bifurcation point after finding the eigenvalues of the associated linearized equation using bifurcation theory and parameter embedding method.[24,25] The eigenvalues that have odd multiplicity are the bifurcation points. Taking Frêchet derivative of Eq. (8), we have the linearized equation

$$\Sigma(p) = \frac{1}{2\pi}\int d|\mathbf{k}| \times\left[\frac{\alpha}{N}\int \frac{dk_0}{\pi}\frac{\Sigma(k)}{k_0^2+\mathbf{k}^2}\frac{1}{(p-k)^2[1+\Pi(|p-k|)]+m_a^2} + g\frac{\Sigma(k)}{p_0^2+\mathbf{k}^2}\right]. \tag{9}$$

For calculational convenience, we made the following scale transformations: $p\to p/\alpha$, $k\to k/\alpha$, and $\Sigma\to\Sigma/\alpha$. An ultraviolet cutoff Λ should be introduced here since the field theory models the physics of high-temperature superconductor only beyond the length scale of lattice constant a ($a\sim\Lambda^{-1}$). To obtain the critical value N_c, we will find the smallest eigenvalue of linearized equation with the help of parameter embedding method.[25]

Numerical computations show that the gauge boson mass m_a and disorder strength g have opposite effects on the critical fermion flavor N_c. The results are shown in Fig. 3 for $r=100$, which is the typical value of Ginzburg parameter of high-temperature superconductor. For any fixed value of g, the critical fermion flavor N_c is rapidly suppressed by growing m_a. For any fixed value of m_a, N_c increases as the disorder strength g increases. In the normal state where $m_a=0$, DCSB takes place for a small mass μ of scalar boson ϕ even when $g=0$. In the superconducting state, as mass $m_a\to 0$, the value N_c coincides with that of the normal state as $\mu\to 0$. Remember that the physical fermion flavor is 2, so chiral symmetry is dynamically broken only when $N_c>2$.

The above results reveal a competition between GSB and DCSB. As a result of this competing relationship, there is a

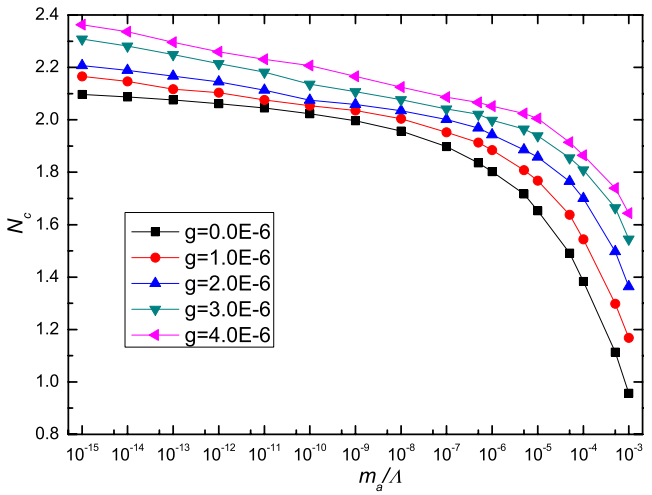

FIG. 3. (Color online) Critical flavor N_c for different values of m_a and g at a ratio of $m_h/m_a=100$.

region for parameters (m_a,g) where these two kinds of symmetry breaking coexist. Since GSB corresponds to superconductivity and DCSB to the formation of long-range antiferromagnetism,[4,26] this describes the competition and coexistence of superconductivity and antiferromagnetism.[10] The effect of disorders is to significantly enhance the occurrence of DCSB and to drive the system toward antiferromagnetism phase.

We now turn to the problem of confinement. The classical potential between two particles with opposite gauge charges can be written in the coordinate space as

$$V(\mathbf{x}) = -e^2 \int \frac{d^2q}{(2\pi)^2} e^{i\mathbf{q}\cdot\mathbf{x}} \frac{1}{q^2[1+\Pi(q^2)]}. \tag{10}$$

It has the following asymptotic form:[13,14]

$$V(\mathbf{x}) = \frac{e^2}{2\pi} \frac{1}{1+\Pi(0)} \ln(e^2|\mathbf{x}|) + \text{const} + \mathcal{O}(|\mathbf{x}|^{-1}). \tag{11}$$

In the absence of vacuum polarization $\Pi(q)$, the potential has a logarithmic form $V(\mathbf{x}) \sim \ln(e^2|\mathbf{x}|)$. This potential increases at large distances and hence is a confining potential. After polarization $\Pi(q)$ is included, the potential depends on $\Pi(0)$. If there is no scalar field, potential $V(\mathbf{x})$ depends on whether the fermion mass is zero or finite. For massless fermion, the vacuum polarization $\Pi(q)=\alpha/8|q|$ diverges as $q\to 0$, so the confining potential is destroyed and the massless fermions are free (deconfined). If the fermion has a constant mass Σ_0 in the DCSB phase, we have

$$\Pi_F(q) = \frac{\alpha}{4\pi q^2}\left(2\Sigma_0 + \frac{q^2-4\Sigma_0^2}{q}\arcsin\frac{q}{\sqrt{q^2+4\Sigma_0^2}}\right).$$

In the limit $q\to 0$, it has a finite value of $\Pi_F(0)=\alpha/8\pi\Sigma_0$. Thus in the DCSB phase, the gauge potential is confining and there is no asymptotic state of fermions.[14]

However, the classical potential $V(\mathbf{x})$ has rather different behavior in the presence of coupling between gauge field and scalar boson. In the GSB state, due to the finite gauge boson mass, the effective polarization function $\Pi(q)$ should be replaced by $\Pi(q)+m_a^2/q^2$. This effective polarization always diverges as $q\to 0$, then the matter fields are always deconfined in the GSB state whether DCSB happens or not. In the gauge symmetric state, the scalar boson has a constant contribution $\Pi_B(0)=e^2/8\pi\mu$ to polarization, so particles are still confined once DCSB happens.

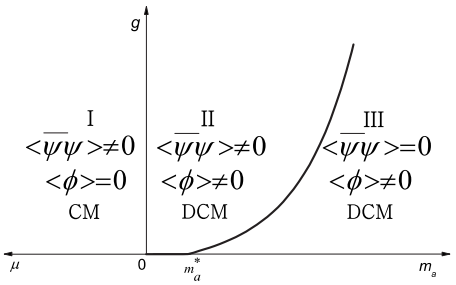

FIG. 4. Phase diagram of the system.

According to the symmetries (chiral and gauge) and the nature of classical potential $V(\mathbf{x})$, the interacting system can have three phases: phase I is characterized by local gauge symmetry, DCSB, and CM; phase II is characterized by GSB, DCSB, and deconfinement (DCM); and phase III is characterized by GSB, chiral symmetry, and deconfinement. The topological phase diagram of the interacting field theory is presented in Fig. 4. There is a critical line (the bold solid line) separating the DCSB phases (I and II) from the chiral-symmetric phase (III). The intersecting point of the critical line with horizontal axis is m_a^*. In the clean limit, $g=0$, m_a^* is just the critical value of m_a, beyond which DCSB is completely suppressed.

We now discuss how these three phases can by identified by experimentally observable quantities. First of all, the vanishing resistivity can differentiate phases II and III from phase I, but it cannot distinguish phase II from phase III. To completely distinguish the three phases I, II, and III, we should consider observable quantities that can efficiently reflect the behavior of fermions, such as specific heat, spin susceptibility, and thermal conductivity.

Among these observable quantities, we choose to consider the low-temperature dc thermal conductivity κ. At very low temperatures, κ is determined solely by fermions because the boson contribution to κ is proportional to T^3, and hence it can be ignored. The thermal conductivity has distinct behaviors in these three phases. (i) In phase I, the fermions are all confined and cannot transport heat current in the bulk system. Therefore, the thermal conductivity must vanish, $\kappa=0$. (ii) In phase II, the massive fermions are deconfined and hence capable of transporting the heat current. Using the Kubo formula, the thermal conductivity can be readily calculated to the leading order of $1/N$ expansion with the result[27]

$$\frac{\kappa}{T} = \frac{1}{6} N k_B^2 \frac{\Gamma_0^2}{\Gamma_0^2+\Sigma_0^2}, \tag{12}$$

where Γ_0 is the scattering rate produced by disorders and k_B is the Boltzmann constant ($\hbar=c=1$). (iii) In phase III, the fermions are massless and deconfined. In the massless fer-

mion limit, $\Sigma_0=0$, κ reduces to a universal value[28] $\frac{\kappa}{T}=\frac{1}{6}Nk_B^2$, which depends only on fundamental constants and is completely independent of impurity scattering rate. Indeed, this universal value of κ has been observed by transport experiments of optimally doped cuprate superconductors.[29] Expression (12) indicates that fermion mass Σ_0 measures the deviation of κ from the universal value. We now conclude that thermal conductivity κ is an ideal quantity to distinguish phases I, II, and III, provided that the system is not in the limit $\Sigma_0 \gg \Gamma_0$ (where κ is significantly suppressed by Σ_0).

We finally comment on the approximations used in this paper. Here we keep only the leading order of $1/N$ expansion when analyzing the DS equation. Although being very interesting, it is not easy to go beyond the leading order because the whole system contains three kinds of interactions. Including coupled equations of $A(p^2)$ and $\Gamma^{\nu}(k,p)$ will add much complexity to numerical computation due to the impossibility of reducing Eq. (8) to a one-dimensional equation. Moreover, we believe that higher order corrections do not change the qualitative conclusion and the topological phase diagram in the present work.

This work was supported by the National Science Foundations of China under Grant No. 10674122.

[1] P. A. Lee, N. Nagaosa, and X.-G. Wen, Rev. Mod. Phys. **78**, 17 (2006).
[2] I. Affleck and J. B. Marston, Phys. Rev. B **37**, 3774 (1988); L. B. Ioffe and A. I. Larkin, *ibid.* **39**, 8988 (1989).
[3] D. H. Kim, P. A. Lee, and X.-G. Wen, Phys. Rev. Lett. **79**, 2109 (1997).
[4] D. H. Kim and P. A. Lee, Ann. Phys. (N.Y.) **272**, 130 (1999).
[5] W. Rantner and X.-G. Wen, Phys. Rev. Lett. **86**, 3871 (2001).
[6] T. Appelquist, D. Nash, and L. C. R. Wijewardhana, Phys. Rev. Lett. **60**, 2575 (1988).
[7] D. Nash, Phys. Rev. Lett. **62**, 3024 (1989).
[8] E. Dagotto, A. Kocić, and J. B. Kogut, Nucl. Phys. B **334**, 279 (1990).
[9] P. Maris, Phys. Rev. D **54**, 4049 (1996); V. P. Gusynin, A. H. Hams, and M. Reenders, *ibid.* **53**, 2227 (1996); C. S. Fischer, R. Alkofer, T. Dahm, and P. Maris, *ibid.* **70**, 073007 (2004).
[10] G.-Z. Liu and G. Cheng, Phys. Rev. D **67**, 065010 (2003).
[11] P. A. Lee and T. V. Ramakrishnan, Rev. Mod. Phys. **57**, 287 (1985); D. Belitz and T. R. Kirkpatrick, *ibid.* **66**, 261 (1994).
[12] M. Göpfert and G. Mack, Commun. Math. Phys. **82**, 545 (1982).
[13] C. J. Burden, J. Praschifka, and C. D. Roberts, Phys. Rev. D **46**, 2695 (1992).
[14] P. Maris, Phys. Rev. D **52**, 6087 (1995).
[15] The kinetic term for the gauge field a_μ is kept here. For simplicity, we assume an isotropic case where the Fermi velocity v_F and gap velocity v_2 are both equal to unity, $v_F=v_2=1$.
[16] When applied to high temperature superconductors, the Lagragian for scalar boson generally has a nonrelativistic form (Refs. 3 and 4). Here, we write down a relativistic Lagragian for the interaction between gauge field and scalar boson, i.e., the scalar QED_3. The advantage is that the standard field theoretic techniques can be used to discuss Anderson-Higgs mechanism and to calculate Dyson-Schwinger equation.
[17] H. Kleinert and F. S. Nogueira, Nucl. Phys. B **651**, 361 (2003).
[18] H. Jiang, G.-Z. Liu, and G. Cheng, J. Phys. A **41**, 255402 (2008).
[19] Y. Nambu and G. Jona-Lasinio, Phys. Rev. **122**, 345 (1961).
[20] D. J. Gross and A. Neveu, Phys. Rev. D **10**, 3235 (1974); E. Witten, Nucl. Phys. B **145**, 110 (1978).
[21] B. Rosenstein, B. J. Warr, and S. H. Park, Phys. Rep. **205**, 59 (1991).
[22] E. Fradkin, Phys. Rev. B **33**, 3263 (1986); A. W. W. Ludwig, M. P. A. Fisher, R. Shankar, and G. Grinstein, *ibid.* **50**, 7526 (1994); A. A. Nersesyan, A. M. Tsvelik, and F. Wenger, Nucl. Phys. B **438**, 561 (1995); C. Mudry, C. Chamon, and X.-G. Wen, Nucl. Phys. **466**, 383 (1996); S. Guruswamy, A. LeClair, and A. W. W. Ludwig, Nucl. Phys. **583**, 476 (2000); A. Altland, B. D. Simons, and M. R. Zirnbauer, Phys. Rep. **359**, 283 (2002); F. Evers and A. D. Mirlin, Rev. Mod. Phys. **80**, 1355 (2008).
[23] A. Altland and B. D. Simons, *Condensed Matter Field Theory* (Cambridge University Press, Cambridge, England, 2006), Chap. 6.
[24] S.-N. Chow and J. K. Hale, *Methods of Bifurcation Theory* (Springer-Verlag, New York, 1982); H. Kagiwada and R. Kalaba, *Integral Equations via Imbedding Methods* (Addison-Wesley, Reading, MA, 1974).
[25] G. Cheng and T. K. Kuo, J. Math. Phys. **35**, 6270 (1994); **35**, 6693 (1994).
[26] Z. Tešanović, O. Vafek, and M. Franz, Phys. Rev. B **65**, 180511(R) (2002); I. F. Herbut, Phys. Rev. Lett. **88**, 047006 (2002).
[27] V. P. Gusynin and V. A. Miransky, Eur. Phys. J. B **37**, 363 (2004).
[28] P. A. Lee, Phys. Rev. Lett. **71**, 1887 (1993); A. C. Durst and P. A. Lee, Phys. Rev. B **62**, 1270 (2000).
[29] L. Taillefer, B. Lussier, R. Gagnon, K. Behnia, and H. Aubin, Phys. Rev. Lett. **79**, 483 (1997); N. E. Hussey, Adv. Phys. **51**, 1685 (2002).